Metabolism Clinical and Experimental 101 (2019) 153998

Contents lists available at ScienceDirect

Metabolism Clinical and Experimental

journal homepage: www.metabolismjournal.com

Interleukin-1α leads to growth hormone deficiency in adamantinomatous craniopharyngioma by targeting pericytes: implication in pituitary fibrosis

Jian Mao [a,1], Binghui Qiu [a,1], Fen Mei [a], Fan Liu [a], Zhanpeng Feng [a], Jun Fan [a], Jing Nie [a], Lijun Huang [b], Xixian Liao [b], Zhenhao Wang [b], Jiahui Zeng [b], Zelin Weng [b], Nailiang Zang [b], Songtao Qi [a,*], Yun Bao [a,*]

[a] Department of Neurosurgery, Nanfang Hospital, Southern Medical University, Guangzhou 510515, China
[b] The First School of Clinical Medicine, Southern Medical University, Guangzhou 510515, China

ARTICLE INFO

Article history:
Received 9 July 2019
Accepted 20 September 2019

Keywords:
Adamantinomatous craniopharyngioma
Interleukin-1α
Pericytes
Pituitary fibrosis
Growth hormone deficiency

ABSTRACT

Background: The incidence of growth hormone deficiency (GHD) in adamantinomatous craniopharyngioma (aCP) is significantly higher than in other sellar region tumors, but the possible mechanism is still elusive. A high level of inflammatory responses is another feature of aCP. We investigated the internal connection between interleukin-1α (IL-1α) and GHD, while focusing on its biological activities in pituitary fibrosis.

Materials and methods: To diagnosis of GHD, the Body Mass Index (BMI), Insulin Like Growth Factor-1(IGF-1) and peak growth hormone (GH) values after insulin stimulation test of 15 aCP patients were recorded. Histological staining was performed on the aCP samples. Levels of 9 proinflammatory cytokines in tumor tissue and cell supernatant were detected using Millipore bead arrays. The effect of IL-1α on GH secretion was evaluated in vivo and in vitro. Western blot, qRT-PCR and cell functional assays were used to explore the potential mechanism through which IL-1α acts on GH secretion. The stereotactic ALZET osmotic pump technique was used to simulate aCP secretion of proinflammatory cytokines in rats. Recombinant IL-1α (rrIL-1α) and conditioned media (CM) prepared from the supernatant of aCP cells was infused directly into the intra-sellar at a rate of 1 μl/h over 28 days, and then the effects of IL-1α treatment on pathological changes of pituitary gland and GH secretion were measured. To further confirm whether IL-1α affects GH secretion through IL-1R1, an IL-1R1 blocker (IL-1R1a, 10 mg/kg body weight, once daily) was administered subcutaneously from the first day until day 28.

Results: There was a significant positive correlation between pituitary fibrosis and GHD ($rS = 0.756$, $P = 0.001$). A number of cytokines, in particular IL-1α, interleukin-8 (IL-8), and monocyte chemoattractant protein-1 (MCP-1), were elevated in tumor tissue and cell supernatant. Only IL-1α showed a significant difference between the GHD group and the No-GHD group ($P < 0.001$, $F = 6.251$ in tumor tissue; $P = 0.003$, $F = 1.529$ in cell supernatant). IL-1α significantly reduced GH secretion in coculture of GH3 and pericytes. The activation of pericytes induced by IL-1α was mediated by the IL-1R1 signaling pathway. In vivo, IL-1α induces pituitary fibrosis, further leading to a decreased level of GH. This pathological change was antagonized by IL-1R1a.

Conclusion: This study found that the cross talk between aCP cells and stroma cells in the pituitary, i.e. pericytes, is an essential factor in the formation of GHD, and we propose that neutralization of IL-1α signaling might be a potential therapy for GHD in aCP.

Abbreviations: GHD, growth hormone deficiency; aCP, adamantinomatous craniopharyngioma; IL-1α, Interleukin-1α; CM, conditioned media; IL-8, interleukin-8; MCP-1, monocyte chemoattractant protein-1; GH, growth hormone; MRI, magnetic resonance imaging; IGF-1, insulin like growth factor-1; BMI, Body Mass Index; IFN-γ, Interferon-γ; IL-1β, Interleukin-1β; IL-6, Interleukin-6; IL-10, Interleukin-10; MIP-1α, Macrophage Inflammatory Protein-1α; TNF-α, Tumor necrosis factor-α; PBS, phosphate-buffered saline; H&E, Haematoxylin and eosin; rrIL-1α, recombinant IL-1α; GAPDH, glyceraldehyde-3-phosphate dehydrogenase; PVDF, polyvinylidene difluoride; CCK-8, Cell counting kit-8; OD, optical density; ELISA, Enzyme-linked immunosorbent assay; ANOVA, one-way analysis of variance; LSD, least significant difference; α-SMA, alpha-smooth muscle actin; NT siRNA, non-targeting small interfering RNA.

* Corresponding authors.
E-mail addresses: qisongtaonfyy@126.com (S. Qi), baoyun519@126.com (Y. Bao).

[1] Jian Mao and Binghui Qiu contributed equally to this work

1. Introduction

Adamantinomatous craniopharyngioma (aCP), originating from the remnants of Rathke's pouch, is an embryonic malformation of the sellar and parasellar regions [1]. Hypopituitarism is more frequent in aCP than other sellar tumors, especially in growth hormone deficiency (GHD) [2–4].

Hypopituitarism is defined as a documented biochemical deficiency in one or more endocrine axes with related pituitary pathology [5]. The syndrome of GHD in adulthood has been fully defined [6,7] and is

https://doi.org/10.1016/j.metabol.2019.153998
0026-0495/

characterized by alterations in body composition, decreased capacity for exercise and quality of life, and a series of unfavorable changes in cardiovascular function [8]. Previously, pituitary and portal vessels compressed by tumor were the main reasons for GHD [9–11]. However, Arrafah et al. [12] found that endocrine levels were not absolutely associated with tumor size. Therefore, the mechanism of GHD in aCP needs to be further studied.

One important difference between aCP and other sellar tumors is that aCPs secrete a variety of proinflammatory cytokines [13]. We have previously found that brain tissue close to aCP is infiltrated by the presence of tumor cell-derived proinflammatory cytokines, which may generate an inflammatory microenvironment [14]. The role of the inflammatory response in the pituitary was first evaluated in human lymphocytic hypophysitis from autopsy as early as 1978 [15]. The inflammatory response is intrinsically involved in GHD [16–18]. Therefore, GHD occurring in aCP is likely to be associated with the inflammatory response in the pituitary.

The inflammatory response often leads to organ dysfunction by inducing fibrosis [19]. Sano et al. [20] found pituitary fibrosis at autopsy in the elderly, which may lead to a reduction in the number of somatotropic cells. Because of the intra-sellar location and aggressive local to surrounding tissues, gross total resection of aCP sometimes involves partial pituitary tissue [1,21].

According to the findings above, we hypothesized that certain proinflammatory cytokines secreted by aCP induce pituitary fibrosis and GHD by promoting the activation of pericytes in the pituitary gland [22]. It is of vital importance to clarify the mechanism of GHD in aCP. Furthermore, we can use antifibrotic drugs and anti-inflammatory drugs to improve growth hormone (GH) function.

2. Materials and methods

2.1. aCP patients

Fifteen specimens of both aCP and pituitary tissue were used in this study. Specimen were collected from patients (age, 25 to 65 years; mean age, 42.53 ± 11.99 years) who underwent gross total resection of aCP at Nanfang Hospital of Southern Medical University (Guangzhou, China) from September 3, 2017 to January 4, 2018. Additionally, aCP was histologically confirmed by two pathologists who independently investigated the samples. A brain magnetic resonance imaging (MRI) scan was performed on all patients. The study was approved by the medical ethics committee of Nanfang Hospital, Southern Medical University, and patients consented to the use of their tissues for the study.

2.2. Diagnosis of GHD

The Body Mass Index (BMI), Insulin Like Growth Factor-1(IGF-1) and peak GH values after insulin stimulation test of all patients were recorded. Diagnosis of GHD was defined by a peak GH value <3 μg/L after effective stimulation based on an insulin stimulation test, or <11 μg/L if BMI was below 25 kg/m^2, <8 μg/L if BMI was between 25 and 30 kg/m^2 and <4 μg/L if BMI was over 30 kg/m^2 to arginine +GHRH test [23].

2.3. MRI protocols

All imaging was performed with a 3.0-T MRI system (Achieva, Philips Healthcare, The Netherlands). A 16-channel body matrix coil was used. The imaging sequences used to evaluate aCP was T1-weighted fluid attenuated inversion recovery (TR, 9000 ms; TE, 120 ms; inversion recovery, 2100 ms). The protocols used for the above sequence was T1-weighted imaging, repetition time (TR), 3.3 ms; echo time (TE), 1.18/2.1 ms; matrix, 384; field of view (FOV), 375 mm × 304 mm × 212 mm; slice thickness, 2.5 mm; slices, 80; and number of signal average (NSA).

2.4. Animals

One hundred twenty Male Sprague–Dawley rats (weight, 135 ± 5 g) were provided by the Laboratory Animal Center of Southern Medical University (Guangzhou, China). They had access to standard chow and water, and were housed under standard laboratory conditions with a 12-h light–dark cycle at room temperature (24 ± 2 °C). Forty-two rats were decapitated for isolating the pericytes. Seventy-eight rats were used for the in vivo experiment.

All animal procedures were approved by the Animal Care Committee of Southern Medical University in accordance with the UK Animal Scientific Procedures Act 1986, the European Union (EU) Directive 2010/63/EU for animal experiments, or the Guide for the Care and Use of Laboratory Animals published by the National Institutes of Health (NIH Publication No. 8023, revised in 1978). The study was approved by the Ethics Committee of Nanfang Hospital (ID: NFYY-2016-117). In addition, all efforts were made to minimize the number of animals used in the study and their suffering.

2.5. Culture of aCP cells

Primary culturing of human aCP cells was assessed according to our previous study [13].

2.6. Measurement of cytokine expression in tissues and cultured cells by Millipore bead arrays

Cytokine levels (Interferon-γ (IFN-γ), Interleukin-1α (IL-1α), Interleukin-1β (IL-1β), Interleukin-6 (IL-6), Interleukin-8 (IL-8), Interleukin-10 (IL-10), monocyte chemoattractant protein-1 (MCP-1), Macrophage Inflammatory Protein-1α (MIP-1α) and Tumor necrosis factor-α (TNF-α)) were measured using Millipore bead arrays according to the manufacturer's instructions. aCP tissues were washed with 2 mL of sterile 1 × PBS, collected by centrifugation and stored in liquid nitrogen for further analysis. Tissues and supernatants of aCP cells were incubated in lysis buffer (1% NP-40, 1% Triton X-100, 0.1% SDS) and centrifuged at 10,000 rpm for 10 min. Total protein concentrations were measured using a Bio-Rad DC kit (Bio-Rad Laboratories, Hercules, CA, USA), and 30 μg of protein was analyzed using the MILLIPLEX MAP Human Cytokine/Chemokine kit (Millipore, Billerica, MA, USA).

2.7. Histology analysis

aCP or rat pituitary samples were prepared as previously described [24]. The sections were incubated overnight at 4 °C with anti-IL-1α (1:100; A2170, ABclonal, Wuhan, China), anti-GH (1:200; 55243-1-AP; Proteintech, Chicago, IL, USA), and anti-alpha-smooth muscle actin (α-SMA, 1:200; ab5694; Abcam, Cambridge, UK). Following washing with phosphate-buffered saline (PBS), the slides were incubated with HRP-goat anti-rabbit IgG (1:500; AS014; ABclonal, Wuhan, China). Haematoxylin and eosin (H&E) staining and Masson's trichrome staining were performed according to standard procedures to detect fibrosis. Positive size was quantified in the section containing the pituitary gland region using ImageJ software, based on Masson's trichrome staining or immunohistochemistry.

2.8. Isolation and treatment of pericytes

Rats were decapitated after inhalation anesthesia with isoflurane to obtain the whole pituitary. Anterior pituitary lobes were dissociated into single cells using successive incubations in 0.25% trypsin-EDTA. For pericytes, freshly dissociated cells were cultured in Dulbecco's modified Eagle medium, containing 10% fetal bovine serum at 37 °C

and 5% CO_2 until pericytes crawled out. In experiments involving administration of conditional medium (CM, 10 ng/mL of IL-1α), rat recombinant IL-1β (10 ng/mL; Z03014-10; Genscript, Shanghai, China), rat recombinant IL-1α (10 ng/mL; Z03115-50; Genscript, Shanghai, China) [25], or rat recombinant IL-1R1a (100 ng/mL; R&D Systems, Minneapolis, MN, USA) [26], 2.5×10^6 cells were cultured for 72 h before treatment. Subsequently, the medium was replaced with serum-free medium containing the indicated treatment for 48 h. Each experiment was repeated three times.

2.9. RT-qPCR

Total RNA was extracted from pericytes using RNAiso Plus reagent (9108, TaKaRa Bio Inc., Tokyo, Japan) according to the manufacturer's instructions. The quantity and concentration of RNA were assessed by measuring absorbance with a spectrophotometer at A260/280. The reverse transcription reactions were performed using a PrimeScript RT reagent kit (RR047A; TaKaRa Bio Inc., Tokyo, Japan). RT-qPCR was performed with a SYBR Premix Ex Taq kit (RR420A; TaKaRa Bio Inc., Tokyo, Japan) on an ABI 7500 real-time PCR system (Applied Biosystems, Foster City, CA, USA) following the manufacturer's instructions. The relative expression levels of each sample were calculated using the $2^{-\Delta\Delta Ct}$ method with glyceraldehyde-3-phosphate dehydrogenase (GAPDH) as the endogenous control. Each experiment repeated was three times. The primer sequences used in qPCR were as follows: IL-1R1 forward: 5′-TGAAAGTGCTACTTGGGTTCATTTG-3′ and reverse: 5′-CATTTGGATACTCCGTGCATTTG-3′; GAPDH forward: 5′-GGCACAGTC AAGGCTGAGAATG-3′ and reverse: 5′-ATGGTGGTGAAGACGCCAGTA-3′.

2.10. Western blot

Western blot analyses were performed with an SDS-PAGE electrophoresis system. Briefly, total extracted pericytes or tissue was lysed with RIPA buffer containing protease inhibitor and protein phosphatase inhibitors at 4 °C for 30 min. The protein concentration was determined using a BCA assay kit (Beyotime Inc., China). Protein samples were separated using SDS-PAGE gel and electro-transferred to polyvinylidene difluoride (PVDF) membranes (Millipore, USA). Then, the membranes were blocked with 5% bovine serum albumin and then incubated with primary antibodies overnight at 4 °C. On the next day, after washing with TBST, membranes were reacted with the corresponding horseradish peroxidase-conjugated secondary antibodies for 1 h at room temperature. Finally, signals were detected using enhanced chemiluminescence reagents and images were captured with a digital camera (Pierce, Rockford, IL, USA). The total gray value of each band was quantified with ImageJ software (NIH), which was normalized to the loading control. Each experiment was repeated three times. The following primary antibodies were used: anti-collagen type I (1:100; abs131984a; Absin Bioscience Inc., Shanghai, China), anti-collagen type III (1:100; abs131560a; ABsin, Shanghai, China), anti-α-SMA (1 μg/mL; ab5694; Abcam, Cambridge, UK), anti-IL-1R1 (1:500; sc-393,998; Santa Cruz Biotechnology, Inc., Dallas, TX, USA), anti-P-p38 MAPK (1:1000; #4511; Cell Signaling Technology, Danvers, MA, USA), anti-p38 MAPK (1:1000; #8690; Cell Signaling Technology, Danvers, MA, USA), anti-P-NFκB p65 (1:1000; #532301; Novus Biologicals, Colorado, USA), anti-NFκB p65 (1:1000; #6956; Cell Signaling Technology, Danvers, MA, USA), and anti-GAPDH (1:5000; AC033; ABclonal, Wuhan, China). HRP goat anti-mouse IgG (1:2000; AS003; ABclonal, Wuhan, China) or HRP goat anti-rabbit IgG (1:2000; AS041, ABclonal; Wuhan, China) was used as a secondary antibody.

2.11. The siRNA transfection of pericytes

The siRNA transfection was done using Lipofectamine RNAiMAX Transfection Reagent (Life Technologies, Carlsbad, CA, USA) in accordance with the manufacturer's protocol. Briefly, 2.5×10^5 pericytes were plated in six-well plates, and the transfection complex (containing 5 μl of Lipofectamine RNAiMAX Transfection Reagent, and 100 μM of siRNAs) was added to cells after 24 h later. After another 72 h, transfected cells were analyzed for RNA expression by RT-qPCR. All experiments were performed within 6 days post-transfection. The siRNA sequences were as follows: si-IL-1R1 forward: 5′-GCAGGUGGAGUUUC CCAAATT-3′ and reverse: 5′-UUUGGGAAACUCCACCUGCTT-3′; NT siRNA forward: 5′-UUCUCCGAACGUGUCACGUTT-3′ and reverse: 5′-ACGUGACACGUUCGGAGAATT-3′. NT siRNA does not target any gene, was used as the negative control.

2.12. Cell counting kit-8 (CCK-8) assay

The CCK-8 (Dojindo, Kumamoto, Japan) assay was used to determine cell proliferation. Briefly, a total of 8×10^3 pericytes per well were seeded into 96-well plates. A group without cells served as the blank. At hours 0, 6, 12, 24 and 48, 10 μL CCK-8 solution was added to cells in each well, followed by incubation at 37 °C for 30 min. The absorbance was measured at 450 nm on a microplate reader and the difference between the optical density (OD) of the cells in medium minus the absorbance of the blank medium-only wells represented the survival/proliferation of cells. With time on the horizontal axis and OD on the vertical axis, we drew a curve of cell activity under the different conditions. Each experiment was repeated three times.

2.13. Migration assay

Cell migration was assessed using a Boyden chamber assay. For these experiments, 1×10^5 pericytes were seeded onto the upper well of a Costar Transwell chamber (8 μM; Corning Life Sciences, Tewksbury, MA, USA) in Dulbecco's modified Eagle medium. The latter were seeded in serum or serum-free medium, which was replaced with 10% fetal bovine serum-containing medium after 24 h. Cells that had migrated to the bottom side of the membrane were fixed in 70% ethanol and stained with Giemsa stain solution 48 h after plating. After staining, nonmigrated cells in the upper chamber were removed using a cotton-tipped applicator. The membranes were mounted onto object slides, and six random fields per slide were counted with a ×10 or ×20 lens objective. Each experiment was repeated three times.

2.14. Scratch wound healing assay

Migration of pericytes was assessed according to the method of Rodriguez et al. [27] with modification. Briefly, 2×10^5 cells were seeded into 3 mm culture dishes in 2 mL of Dulbecco's modified Eagle medium supplemented with 10% fetal bovine serum and antibiotics. The cells were maintained at 37 °C and 5% CO_2 until confluence. Once confluent, each dish of monolayer cells was given a mechanical wound by scoring with a 200 μL pipette tip, parallel to the grid bars and the central grid line. This facilitated easy observation of the cells growing back together. Wound placement was checked with a Leica microscope (LEICA DMI3000 B; Wetzlall, Germany). The medium was then removed, and the cells were washed 5 times with PBS, and then replaced with CM or rrIL-1α treatment. Two groups of wells were pretreated with IL-1R1a for 24 h and then washed 5 times with PBS. Cells in each dish along the induced wound were photographed at 0 and 48 h using a digital camera (Olympus, Tokyo, Japan; magnification, 5×) attached to a light microscope. ImageJ (National Institutes of Health, Bethesda, MD, USA) software was used to measure the area of initial damage (images were taken at time 0) and of the remaining damage after 48 h. The percentage of wound repair was then calculated. Each was experiment repeated three times.

2.15. Isolation and treatment of somatotropic cells

Primary culturing of somatotropic cells was assessed according to our improved method [28]. Cells were stabilized after 3 days, and 10 ng/mL rrIL-1α was added for 48 h. The changes in the culture system were examined with an inverted microscope (Leica DMI3000 B microscope, magnification, 200×). Each experiment was repeated three times.

2.16. Immunofluorescence

Somatotropic cells or pericytes were prepared in accordance with the manufacturer's protocol. Then, cells were incubated overnight at 4 °C with the following antibodies diluted in 5% BSA blocking solution: anti-GH (1:100; sc-166696, Santa Cruz Biotechnology, Inc., Dallas, TX, USA) and anti-Pit-1 (1:100; sc-25258, Santa Cruz Biotechnology, Inc., Dallas, TX, USA), which were used to identify somatotropic cells; and anti-desmin (1:50; ab32362; Abcam, Cambridge, UK) and anti-α-SMA (1:100; ab5694; Abcam, Cambridge, UK), which were used to identify pericytes and myofibroblasts. After three washes with PBS for 10 min, samples were stained for 1 h at room temperature with fluorescent secondary antibodies (1:1000, KGAB011 or KGAB013, KeyGEN BioTECH, Nanjing, China) followed by 5 min of DAPI (KGR0001, KeyGEN BioTECH, Nanjing, China) staining for nucleus visualization. Cells were observed under a spinning-disc confocal microscope (10i, Olympus, Tokyo, Japan, magnification, 1000×).

2.17. Preparing the CM

A total of 1×10^6 aCP cells were initially seeded in the petri dish. Cells were serum/hormone-deprived overnight when fully confluent by the next day. Cell-free supernatant was collected and analyzed by Enzyme-linked immunosorbent assay (ELISA). To achieve an applicable concentration of IL-1α, the cell-free supernatant was concentrated using a Thermo Scientific Pierce Protein Concentrator (10 K MWCO, 88535, Thermo Scientific Fisher, Waltham, MA, USA).

2.18. Coculture model

GH3 (rat somatotropic) cells and pericytes were used in the coculture experiment. Briefly, pericytes were plated on 1.0-μM-pore 24-well cell culture inserts (MCRP24H48, Millipore, Billerica, MA, USA), and GH3 cells were seeded on 24-well plates. When both cell layers were confluent, the Transwell insert with pericytes was cocultured with the GH3 cells and left for 72 h.

2.19. Rat experiments

Oblique puncture was conditionally used to avoid the upper sagittal sinus. Under inhalation anesthesia by isoflurane (970-00026-00; RWD Life Science, Shenzhen, China), rats were shaved, and the scalp was opened for approximately 20 mm along the midline of the sagittal plane and then fixed in an ultra-precise stereotaxic apparatus (900–00035-00; RWD Life Science Inc., San Diego, CA, USA) to the coordinates of 4 mm posterior to the bregma and 1.4 mm lateral to the midline with continuous inhalation anesthesia. IL-1α and CM were injected at a rate of 1 ul/h over 28 days through the cannula and an injector connected to an infusion pump (DURECT Corp, Cupertino, CA, UAS). The cannula was inserted intracranially for 10.2 mm at 8° to the brain sagittal plane, then fixed by dental cement (Fig. 1). Recombinant IL-1R1a (10 mg/kg body weight, once daily) was administered subcutaneously from the first day until day 28, thereby allowing a washout period of 5 days. Rats were free to move throughout this time. Data on body weight, body length, and tail length were collected on days 0 and 28. The peripheral blood was drawn by retro-orbital bleeding after 32 days.

2.20. ELISA

Peripheral blood was drawn from rats by retro-orbital bleeding in the amount of 1 mL and was kept at ambient temperature for 30 min, followed by centrifugation at 3000 rpm for 10 min. Serum was used immediately for ELISA. Samples were diluted and subjected to standard ELISA to determine GH levels in accordance with the manufacturer's protocol (Rat/mouse GH ELISA kit, EZRMGH-45K; Millipore, Billerica, MA, USA; sensitivity: minimum of 0.07 ng/mL when using a 10 μL sample size; specificity: 100%).

2.21. Statistical analysis

Results are expressed as mean ± SD or mean ± SEM from at least three independent experiments by using GraphPad Prism 5 or SPSS 19.0 software (IBM, Armonk, NY, USA). Statistical analysis was conducted by using an unpaired Student's *t*-test or one-way analysis of variance (ANOVA) followed by the least significant difference (LSD) post hoc-test. A two-tailed probability value of <0.05 was considered statistically significant. * represents $P < 0.05$; ** represents $P < 0.01$; *** represents $P < 0.001$.

3. Results

3.1. aCP patients with GHD have pituitary fibrosis

All 15 patients were dynamically tested for GHD before surgery. Peak GH levels after the GHRH + arginine test were statistically lower in GHD patients. In particular, 10/15 (66.7%) patients, four females and six males, had GHD, while 5/15 (33.3%) patients showed a normal GH peak and were considered to have normal GH secretion (Table 1).

Representative preoperative MRI showed that the pituitary glands were compressed by the tumors (Fig. 2A). In GHD patients, the aCP pushed part of the pituitary gland downward to the left. The boundary between tumors and the pituitary was clear, and no tumor invasion was observed. In the No-GHD patients, the calcified tumor pushed part of the pituitary to the upper left. Due to tumor compression, glandular cells lost their normal cordlike arrangement structure (Fig. 2B).

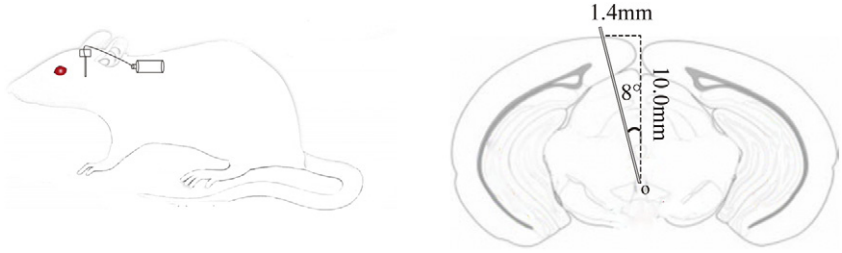

Fig. 1. Diagram showing the stereotactic ALZET Osmotic Pumps.

Table 1
Comparison of anthropometric and biochemical parameters between the GHD and the No-GHD patients.

Parameters	GHD	No-GHD	P value
Number of patients	10	5	
Sex (F/M)	4/6	3/2	
Age (years)	41.50 ± 11.44	44.6 ± 14.15	ns
BMI	22.05 ± 3.02	21.73 ± 2.46	ns
peak GH (μg/L)	0.47 ± 0.37	6.66 ± 1.60	0.0008
IGF-1 (μg/L)	97.04 ± 19.51	252.82 ± 44.32	<0.0001

ns: not significant.

Table 2
Correlation analysis of the number of GHD patients and pituitary fibrosis.

			GHD	FP
Spearman's rho	GHD	Correlation	1.000	0.756**
		Sig. (2-tailed)	–	0.001
		N	15	15
	FP	Correlation	0.756**	1.000
		Sig. (2-tailed)	0.001	–
		N	15	15

FP: Fibrotic pituitary.
** Correlation is significant at the 0.01 level (2-tailed).

Typical fibrotic changes happened in GHD patients, which led to a decrease in parenchyma cells in the pituitary gland, while fibrous connective tissue significantly increased, especially around the sinusoidal capillary wall. No pituitary fibrosis was observed in the No-GHD patients (Fig. 2C–D). In this study, pituitary fibrosis was found in 80% of the specimens of the GHD group (Table 2). There was a significant positive correlation between pituitary fibrosis and GHD ($r_S = 0.756$, $P = 0.001$).

3.2. IL-1α is associated with GHD

We first tested whether the increased levels of proinflammatory cytokines in aCP observed previously [14] would be associated with GHD. As shown in Fig. 3A, of the 9 cytokines tested, IL-1α, IL-8, and MCP-1 were expressed significantly higher than other cytokines. Only IL-1α showed a significant difference between the GHD group and the No-GHD group ($P < 0.001$, $F = 6.251$ in tumor tissue; $P = 0.003$, $F = 1.529$ in cell supernatant). No significant correlations between other cytokines (IFN-γ, IL-1β, IL-6, IL-8, IL-10, MCP-1, MIP-1α, and TNF-α) and GHD were found.

Immunohistochemistry shows that tumors had stronger IL-1α expression both in tumors and in pituitary in the GHD group compared to the No-GHD group. Similarly, the expression of α-SMA was higher in the pituitary gland in the GHD group, especially around the sinus capillary wall (Fig. 3B). GH expression was lower in the GHD group, consistent with the endocrine examination results (Table 1). These results suggest that proinflammatory cytokines are elevated in aCP and that IL-1α is related to pituitary fibrosis and GHD.

3.3. IL-1α enhances the viability of pericytes via the IL-1R1 signaling pathway

A previous study on IL-1α signaling highlighted IL-1R1 as a receptor mediating the activity of both the pre and cleaved forms of IL-1α

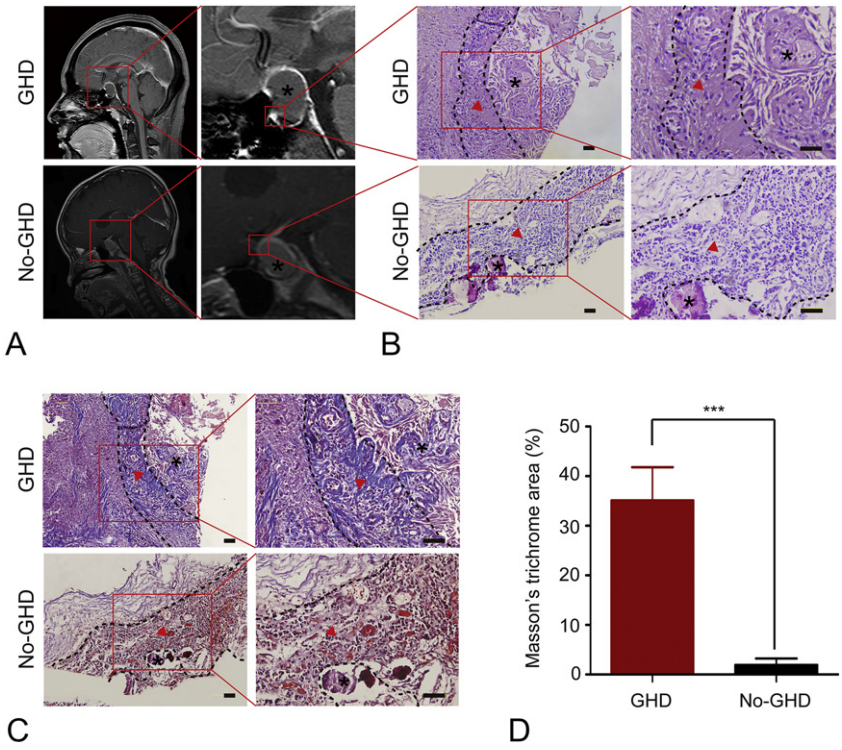

Fig. 2. The different pathological changes of the pituitary gland in aCP patients with or without GHD. (A) Representative sagittal contrast-enhanced MR images of aCP patients with GHD or No-GHD. Black asterisk: tumor. (B) Representative HE staining of the pituitary gland in aCP patients with or without GHD. Red triangle: pituitary area; black asterisk: tumor area. Scale bar = 100 μm. (C) Representative Masson's trichrome staining of the pituitary gland in aCP patients with or without GHD. Marked pituitary fibrosis is shown in GHD (blue). Red triangle: pituitary area; black asterisk: tumor area. Scale bar = 100 μm. (D) Quantification of Masson's trichrome staining is presented. n = 10 in GHD and 5 in No-GHD. GHD: growth hormone deficiency, No-GHD: no growth hormone deficiency. Statistical comparisons were made using two-tailed Student's *t*-test. All data are represented as mean ± SD.

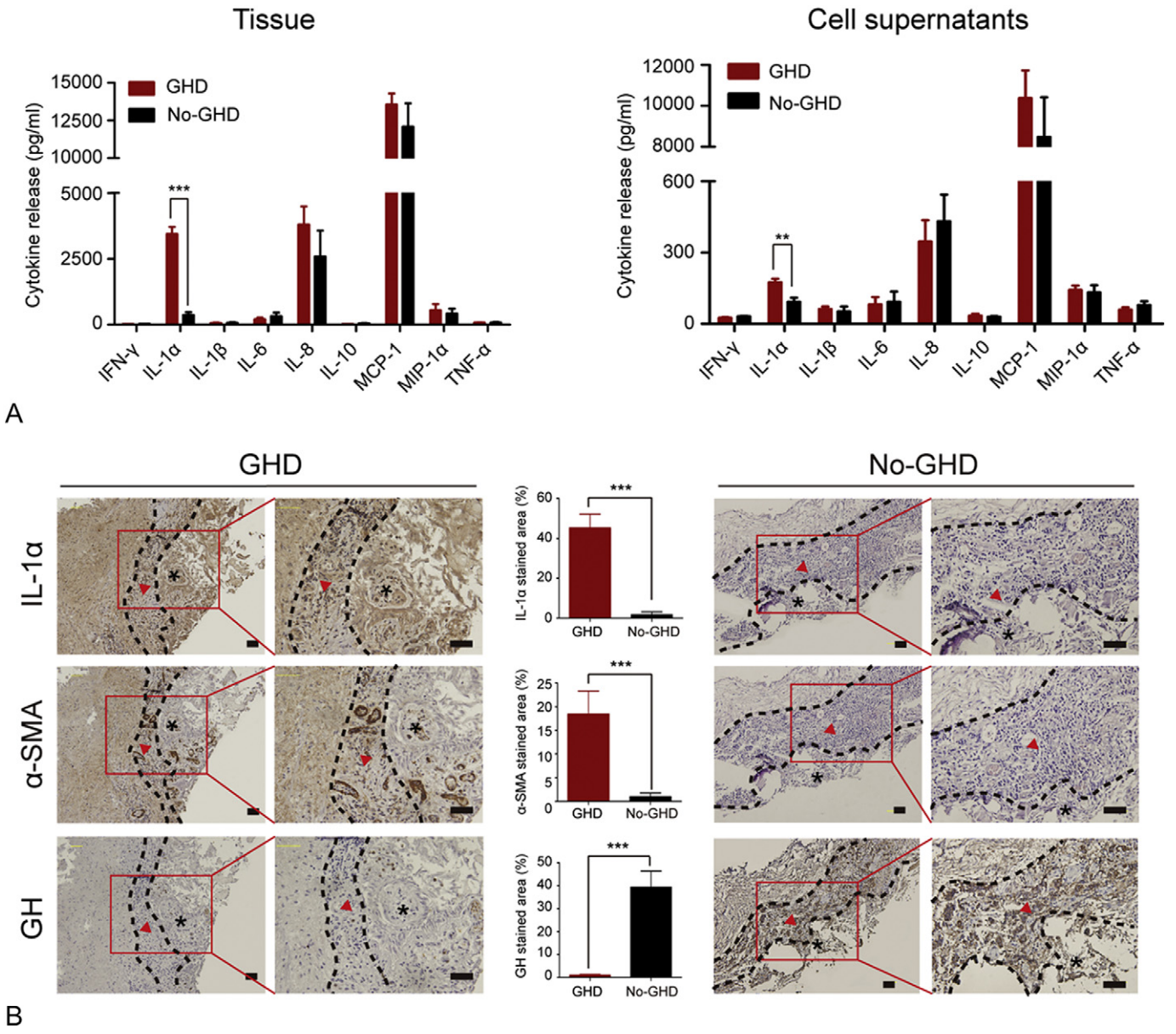

Fig. 3. The correlation between levels of proinflammatory cytokines and GHD. (A) Cytokine levels in aCP tissue or cell supernatants were measured using Millipore bead arrays. Note particularly high levels of expression of IL-1α, IL-8, and MCP-1 in all samples. IL-1α showed the only significant difference between GHD and No-GHD. n = 10 in GHD and 5 in No-GHD. (B) Immunoreactivity of IL-1α and α-SMA is high, but GH is low in GHD. Quantification of staining is presented as positive expression areas. n = 10 in GHD and 5 in No-GHD. Red triangle: pituitary area; black asterisk: tumor area. Scale bar = 100 μm. GHD: growth hormone deficiency, No-GHD: no growth hormone deficiency. Statistical comparisons were made using two-tailed Student's *t*-test. Data are represented as mean ± SEM (B) or mean ± SD (C).

[29]. Analysis of RNA and protein levels showed that IL-1R1 expression gradually became positive in pericytes after administration of 10 ng/mL rrIL-1α for 48 h (Fig. 4A–C).

To confirm the involvement of IL-1R1 in controlling IL-1α biological responses, we transiently transfected pericytes with siRNA against IL-1R1, followed by stimulation with IL-1α. Compared with nontargeting small interfering RNA (NT siRNA), siIL-1R1 transfection pericytes led to an 80% decrease in the overall expression of IL-1R1, which was validated at the RNA and protein levels (Fig. 4D–F).

Kyoto Encyclopedia of Genes and Genomes pathway maps [30] show p38 MAPK and NFκB signaling as the downstream pathways of IL-1R1 (www.kegg.jp/dbget-bin/www_bget?mmu:16177). Previous studies have shown that fibrosis is involved in the p38 MAPK signaling pathway [31]. We found that phosphorylation of p38 MAPK was increased within 48 h when pericytes were stimulated with 10 ng/mL rrIL-1α, and this was prevented by knocking down IL-1R1 (Fig. 4G–H). In addition, no NFκB p65 phosphorylation was seen (data not shown). Relevant functional assays were performed to indicate the effects of IL-1α on pericytes. A CCK-8 assay was used to confirm the effect of IL-1α on the proliferative ability of pericytes. The growth rate of pericytes treated with rrIL-1α (NT siRNA + rrIL-1α) was significantly increased compared with the negative control (NT siRNA + PBS), while pretransfection with siRNA against IL-1R1 (siIL-1R1 + rrIL-1α) abolished the effects (Fig. 4I). Matrigel invasion and wound healing assays were used to examine the effects of IL-1α on pericyte migration and invasion. IL-1α enhanced the migration and invasion of pericytes, whereas pre-knocked down IL-1R1 abolished the effects (Fig. 4J–M). Taken together, the results of our biochemical assays suggested that IL-1α enhances the viability of pericytes via the IL-1R1 signaling pathway.

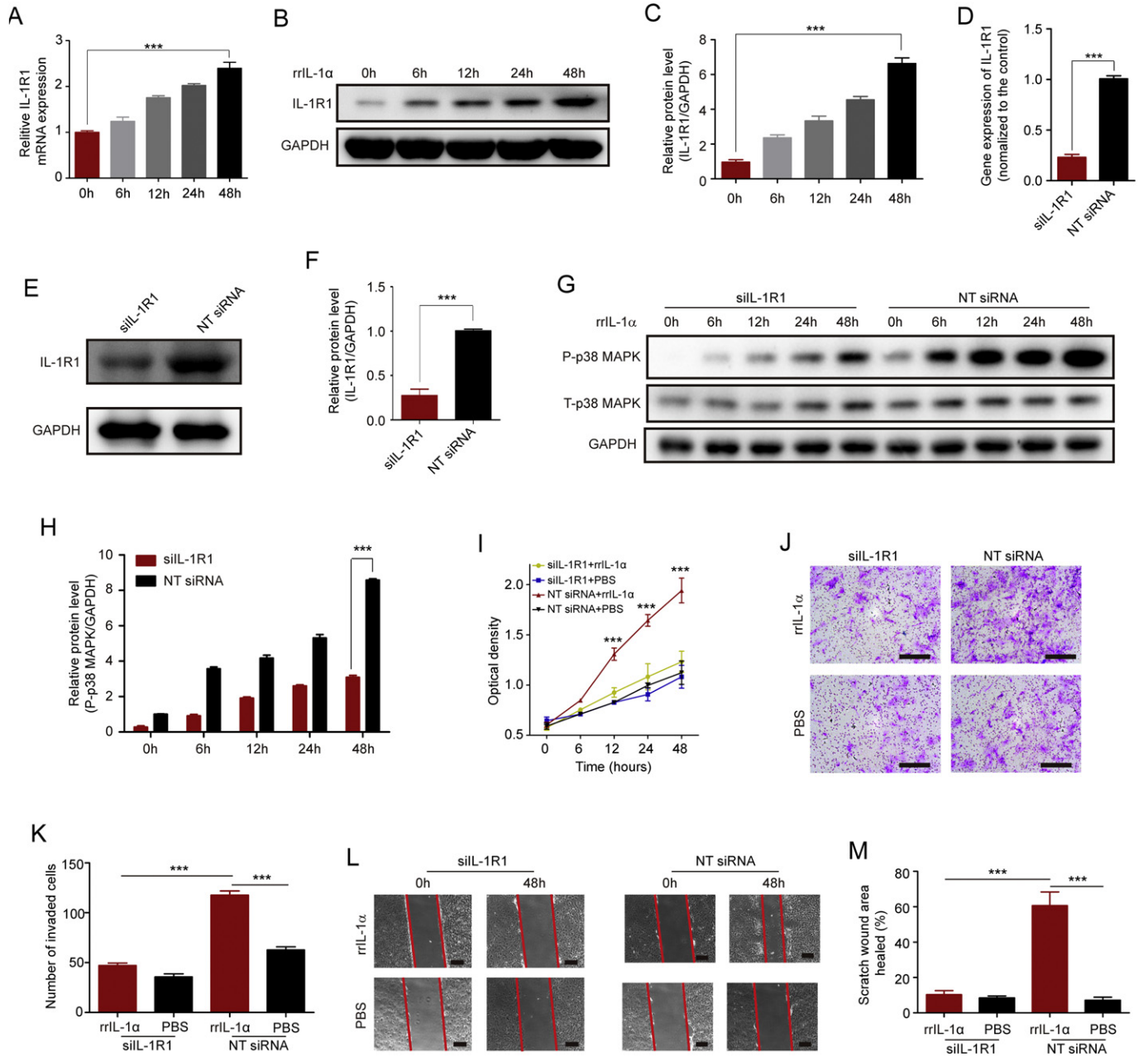

Fig. 4. IL-1α regulates the increased viability of pericytes through the IL-1R1 signal pathway. (A) RT-qPCR of IL-1R1 expression in pericytes treated with rrIL-1α for 0–48 h. (B) Representative western blot analysis of IL-1R1 expression in pericytes treated with rrIL-1α for 0–48 h. GAPDH expression was used to confirm equal protein loading and blotting. (C) The statistical analyses of IL-1R1 in (B) are shown. n = 3 in each group. (D) RT-qPCR of IL-1R1 expression in pericytes treated with siRNA control or siRNA for IL-1R1. Nontargeting siRNA was used as a control. (E) Western blot analysis of IL-1R1 expression in pericytes treated with NT siRNA or siRNA for IL-1R1. GAPDH expression was used to confirm equal protein loading and blotting. (F) The statistical analysis of IL-1R1 in (D) is shown. n = 3 in each group. (G) Pericytes were treated with siRNA for IL-1R1 and then stimulated with 10 ng/mL rrIL-1α for 0–48 h. p38 MAPK signaling was analyzed by western blot. GAPDH expression was used to confirm equal protein loading and blotting. NT siRNA was used as a control. (H) The statistical analysis of IL-1R1 in (G) is shown. n = 3 in each group. (I) CCK-8 analysis of pericytes treated with NT siRNA or siRNA for IL-1R1 after 10 ng/mL rrIL-1α administration. n = 3 in each group. (J) Cell migration analysis of pericytes that were treated with NT siRNA or siRNA for IL-1R1 was evaluated by Boyden chamber assay after administration of 10 ng/mL rrIL-1α. Scale bar = 100 μm. (K) The statistical analysis of the number of invaded pericytes in the cell migration assay is shown. n = 3 in each group. (L) Scratch wound healing assay of pericytes treated with NT siRNA or siRNA for IL-1R1 after administration of 10 ng/mL rrIL-1α. Scale bar = 400 μm. (M) The statistical analysis of the healed scratch wound area of pericytes is shown. n = 3 in each group. Statistical comparisons were made using two-tailed Student's *t*-test (A, C, D, F, H, K and M) or one-way ANOVA with post hoc LSD's test (I). All data are expressed as mean ± SD.

3.4. IL-1α leads to a decrease in GH secretion via activating pericytes

To directly respond to the effect of IL-1α on somatotropic cells, primary somatotropic cells were used for subsequent experiments (Fig. 5A). Microscopically, somatotropic cells markedly decreased and spindle cells appeared after rrIL-1α treatment (Fig. 5B). Pericytes are the main kind of cell producing fibrillar collagens in the pituitary gland [32] and are marked by desmin [33]. Pericytes provide a major source of α-SMA-positive myofibroblasts that are involved in the development of fibrosis [22]. Immunofluorescence analysis confirmed that the spindle cells were pericytes, which could turn into myofibroblasts with IL-1α stimulation (Fig. 5C). IL-1R1a (IL-1R1 blocker) does not distinguish between IL-1α and IL-1β; hence, to further investigate the active role of IL-1α in the

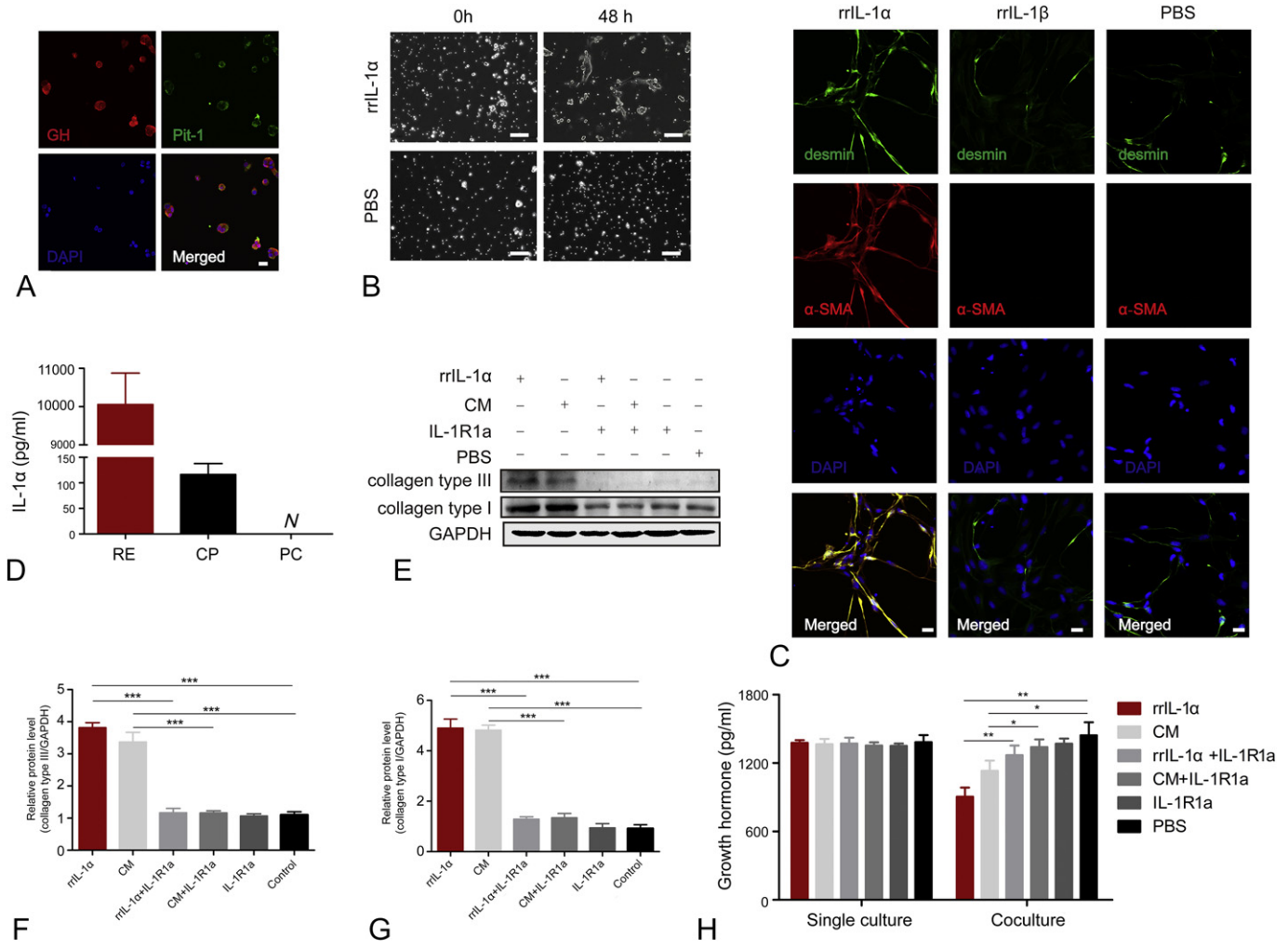

Fig. 5. Pericytes are involved in the change in GH secretion caused by IL-1α in vitro. (A) Immunofluorescence analysis was used to positively identify primary rat somatotropic cells. Scale bar = 20 μm. (B) The proportion of somatotropes decreased with increasing spindle-shaped cells after administration of 10 ng/mL rrIL-1α for 48 h. Scale bar = 100 μm. (C) Immunofluorescence analysis of spindle-shaped cells showed that these spindle-shaped cells were pericytes. rrIL-1β did not activate pericytes. PBS was used as a control. Scale bar = 20 μm. (D) ELISA of IL-1α in aCP cell supernatants. n = 3 in each group. rrIL-1α (10 ng/mL) was used as a positive control. RE: 10 ng/mL of rrIL-1α. CP: supernatant of aCP cells. PC: supernatant of primary somatotropic cells. N: none. (E) Western blot of collagen type I and collagen type III in pericytes after receiving the indicated treatments for 48 h. GAPDH expression was monitored to confirm equal protein loading and blotting. (F-G) The statistical analyses of collagen type I and collagen type III in (E) are shown. n = 3 in each group. (H) ELISA of GH expression in single culture or coculture of GH3 cells after receiving treatments for 48 h. n = 3 in each group. Statistical comparisons were made using two-tailed Student's *t*-test. All data are expressed as mean ± SD.

activation of pericytes, we performed additional experiments using rrIL-1β to treat pericytes. IL-1β did not activate pericytes compared with PBS controls (Fig. 5C).

Next, to further investigate the effects of IL-1α secreted by aCP on pericytes, the concentration of IL-1α in CM was examined by ELISA and was approximately 100 times lower than that of rrIL-1α (Fig. 5D). Pericytes were isolated and treated with CM and rrIL-1α for 48 h. The expression levels of collagen types I and III were significantly enriched when pericytes were treated with CM and rrIL-1α compared with PBS (Fig. 5E–G). Our results showed that pretreatment with IL-1R1a significantly reduced CM-induced collagen synthesis (Fig. 5F–G), which indicates that IL-1α in CM is involved in mediating the potent fibrogenic effects of the pituitary gland.

xWe found that IL-1α had no influence on GH secretion in single culture of GH3 cells. However, they significantly reduced GH secretion in coculture of GH3 cells and pericytes (Fig. 5H). Pretreatment with IL-1R1a prevented rrIL-1α- and CM-induced decreases in GH secretion. Taken together, these results demonstrated that IL-1α decreases GH secretion by activating pericytes in aCP.

3.5. IL-1α induces pituitary fibrosis in vivo

To study the effect of IL-1α on the pituitary gland in vivo, we designed a rat model with infusion to the intra-sellar, which was directed using stereotactic ALZET osmotic pumps. After 32 days, we dissected the pituitary gland for histological staining. As displayed in Fig. 6A, administration of 1 ng/mL rrIL-1α caused mild fibrosis in the pituitary gland, which slightly increased the cordlike fibrous connective tissue. After that, administration of 10 ng/mL rrIL-1α significantly reduced the parenchyma cells in the pituitary gland and increased the cordlike fibrous connective tissue, presenting typical fibrotic changes. α-SMA expression was positive in the pituitary gland, which was stronger at higher concentrations of rrIL-1α (Fig. 6B). Moreover, CM treatment led to obvious fibrosis changes in the rat pituitary gland (Fig. 6C). α-SMA was also highly expressed in the CM group (Fig. 6D). Taken together, the in vivo data led us to conclude that IL-1α is the main cytokine leading to fibrosis of the pituitary gland in the supernatant of aCP cells.

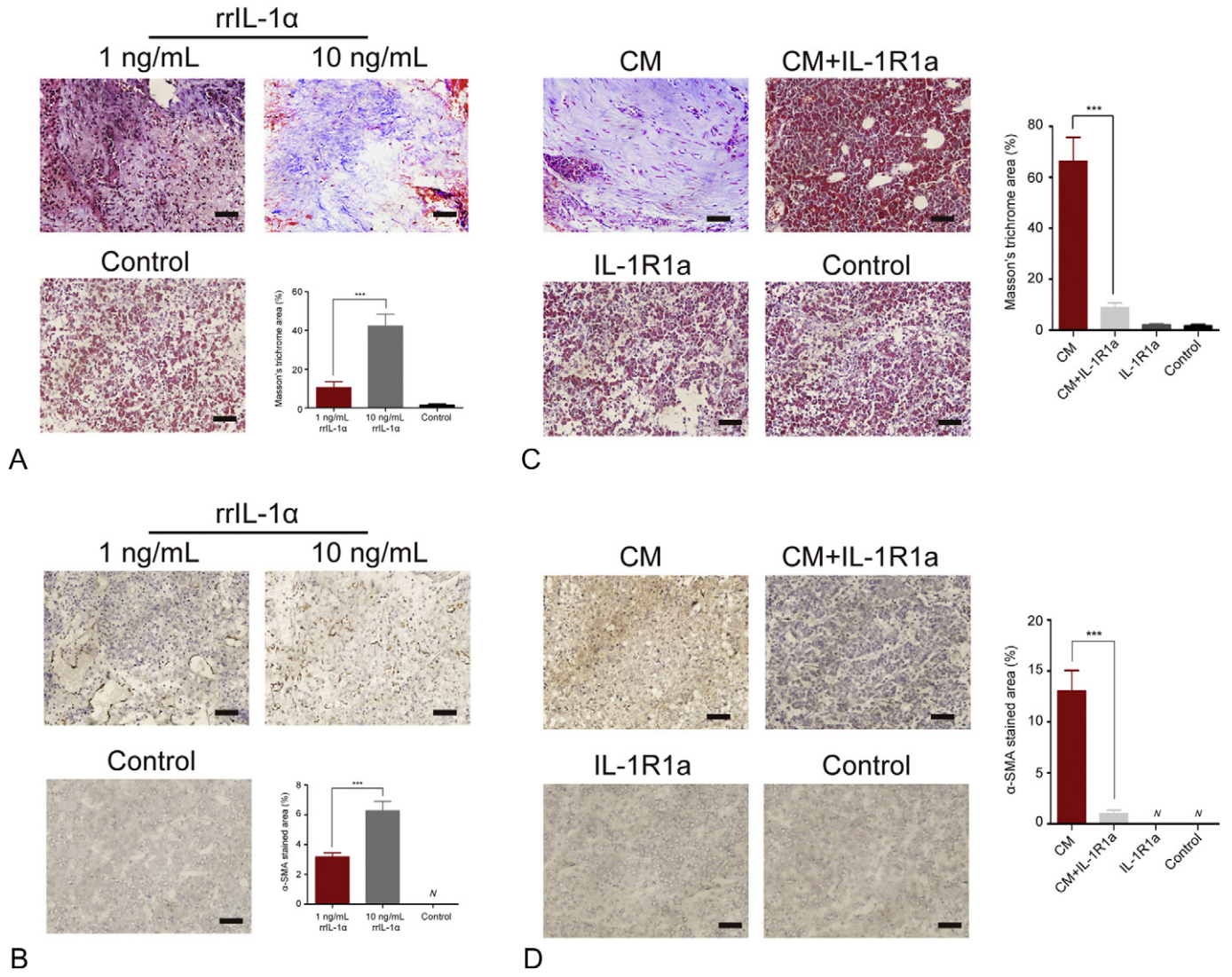

Fig. 6. Diagnostic variation of rat pituitary after IL-1α administration. (A) Masson's trichrome staining showed that administration of both 1 ng/mL and 10 ng/mL rrIL-1α induced pituitary fibrosis (blue). The degree of fibrosis increased with increasing IL-1α concentration. Normal saline (NS) was the control. Quantification of Masson's trichrome staining is presented. n = 6 in each group. Scale bar = 100 μm. (B) Immunohistochemistry analysis confirmed that administration of either 1 or 10 ng/mL rrIL-1α activated the expression of α-SMA. NS was the control. Quantification of staining is presented as positive expression areas. n = 6 in each group. Scale bar = 100 μm. N: none. (C) Masson's trichrome staining showed that CM administration induced pituitary fibrosis(blue), which was prevented by IL-1R1a. NS was the control. Quantification of Masson's trichrome staining is presented. n = 6 in each group. Scale bar = 100 μm. (D) Immunohistochemistry analysis confirmed that CM administration activated the expression of α-SMA, which was averted via IL-1R1a. NS was the control. Quantification of staining is presented as positive expression areas. n = 6 in each group. Scale bar = 100 μm. N: none. Statistical comparisons were made using two-tailed Student's *t*-test. All data are expressed as mean ± SD.

3.6. IL-1α leads to decreased GH level by inducing pituitary fibrosis

To further verify the effects of pituitary fibrosis on GH secretion in vivo, the eye venous blood of rats was collected at 8:00 am after 32 days, and the GH level in serum was detected by ELISA. GH levels in the rrIL-1α and CM groups were significantly decreased compared with the control (Fig. 7A). Pituitary fibrosis significantly inhibited the growth of rats. IL-1α treatment significantly inhibited body weight, body length, and tail length in rats compared with controls. Both rrIL-1α and CM had similar growth retardation effects (Fig. 7B–D). However, IL-1R1a treatment reversed the IL-1α-induced growth retardation.

Notably, the degree of α-SMA expression in the rrIL-1α and CM groups was alleviated under pretreatement with IL-1R1a. Deposition of collagens in the 10 ng/mL rrIL-1α group was significantly higher than in the controls, which was the same as that in the CM group (Fig. 7E–G). Therefore, these results indicated that fibrosis of the pituitary gland caused by IL-1α decreases GH secretion, and this pathological change can be antagonized by IL-1R1a.

4. Discussion

A growing body of evidence points to the importance of GH in the regulation of aging and disease [34]. The incidence of GHD in aCP is very high, at 75% [1]. Here, we found that one of the characteristics of aCP is increased proinflammatory expression, and IL-1α is the key cytokine that causes GHD in aCP.

Different lines of evidence prove that the local inflammatory response can cause tissue fibrosis, which further leads to decreased organ function [35,36]. Current studies on GHD of aCP focus only on tumor compression, that is, the decreased GH secretion caused by mechanical compression of the hypothalamus or pituitary gland by the tumor [9–11]. In this study, we found that there was a significant

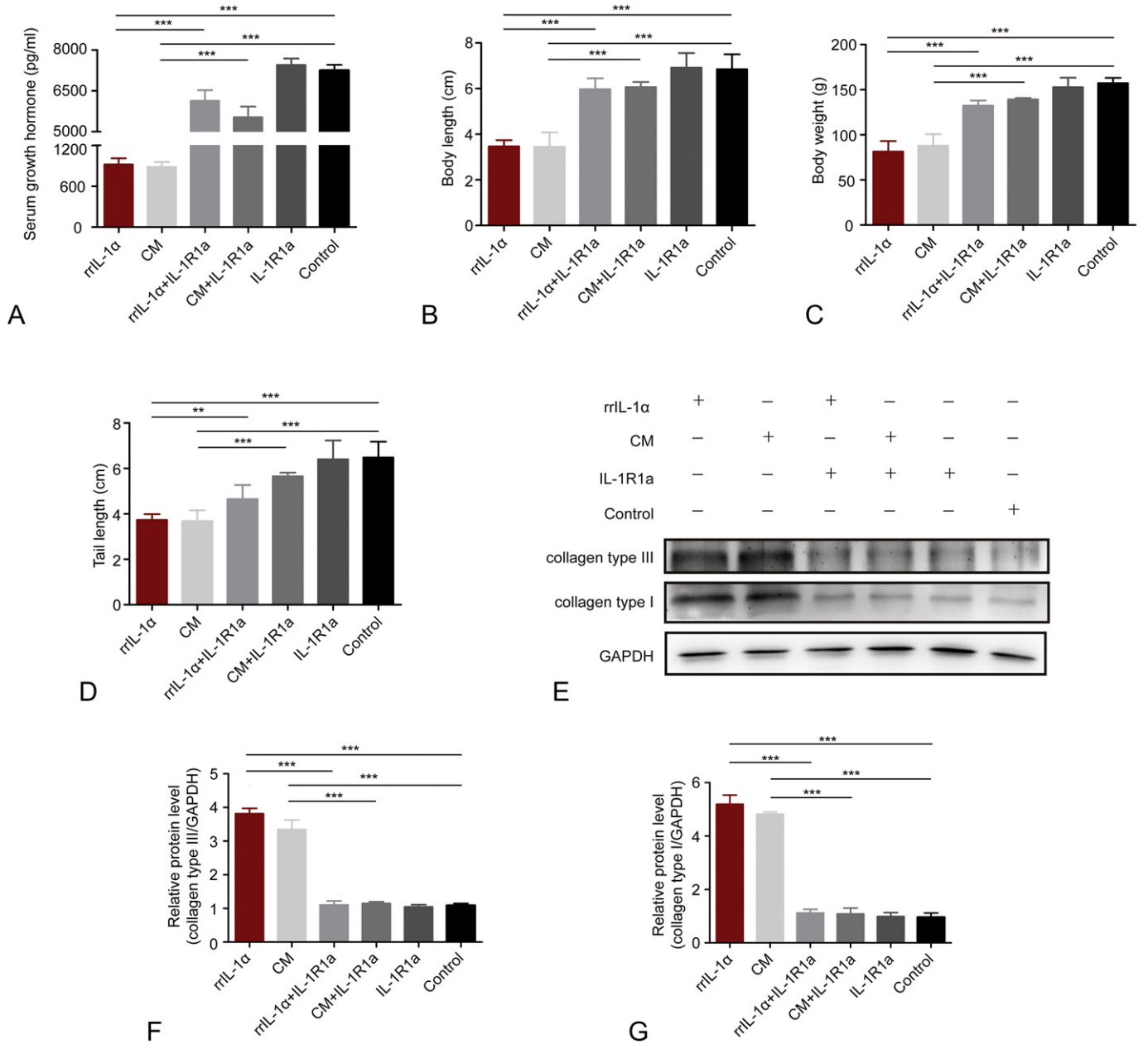

Fig. 7. Pituitary fibrosis can affect growth and development. (A) ELISA of GH expression in peripheral blood after receiving treatments for 28 days. n = 6 in each group. (B–D) Data of body length, body weight, and tail length after receiving treatments for 28 days. NS was the control. n = 6 in each group. (E) Representative western blot analysis of collagen type I and collagen type III in the pituitary. GAPDH expression was used to confirm equal protein loading and blotting. (F–G) The statistical analyses of collagen type I and collagen type III in (E) are shown. n = 6 in each group. Statistical comparisons were made using two-tailed Student's *t*-test. All data are expressed as mean ± SD.

correlation between GHD and pituitary fibrosis. Interestingly, the cytokines we found to be expressed at the highest levels, IL-1α, IL-8, and MCP-1, have been previously shown to be involved in fibrosis. It is hence conceivable that these three cytokines, and likely others we have not specifically analyzed, are at least in part responsible for inducing pituitary fibrosis and the ensuing GHD. Therefore, we divided the samples of these 15 patients into two groups according to the presence or absence of GHD. We found that only IL-1α secretion was significantly different between the GHD and No-GHD groups. The data suggest that IL-1α may be a key factor for GHD through pituitary fibrosis in aCP.

IL-1α is known as a fibroblast-activating factor. It has been demonstrated that IL-1α has mitogenic effects on fibroblasts, mechanistically connecting excessive IL-1α expression with a pathological tissue response, which manifests in excessive accumulation of collagen and fibrosis [37]. Pericytes, also named perivascular fibroblasts, surround the endothelial cells in capillaries and veins [22]. Extracellular matrix components such as collagen types I and III in the anterior pituitary are mainly produced by pericytes [32]. We studied differentiated, activated pericytes isolated directly from rat pituitary glands. Those activated pericytes expressed imprinted phenotypes, in which they were stable during cultivation, and their in vitro behavior likely reflected their function in vivo. Our study lays a foundation for studying the effect of IL-1α on the activation of pericytes.

Although previous studies have suggested that proinflammatory cytokines can promote the endocrine function of the pituitary [38–40], the present study found that IL-1α can inhibit the secretion function of GH3 cells. However, IL-1α did not merely affect the endocrine function of GH3 cells, which was consistent with a previous study

[41]. IL-1α needs to activate pericytes to achieve its ability to suppress GH secretion. We used the stereotactic ALZET Osmotic pump to deliver IL-1α to the pituitary gland of rats, and the serum GH level was significantly decreased, with growth retardation. These results showed that IL-1α can inhibit the endocrine capacity of somatotropic cells in vivo. Moreover, histopathological staining of the pituitary gland revealed extensive fibrosis. Therefore, IL-1α causes a reduction in GH secretion by causing pituitary fibrosis.

We attempted to prevent the fibrosis process by targeting the receptor or downstream signal of IL-1α on the pericytes. IL-1R1a is a specific blocker of IL-1R1, and we designed both in vivo and in vitro experiments with IL-1R1a. As expected, IL-1R1a prevented the fibrosis process in the rrIL-1α group, as well as in the CM group. This result further suggests that IL-1α is a key factor in pituitary fibrosis among various proinflammatory cytokines secreted by aCP, and it was also revealed that IL-1R1 receptor targeting in pericytes has potential value in endocrine therapy for aCP. The most appropriate animal model should be related to aCP formation in the sellar region. However, since this model has not been developed yet, we could only use the stereotactic ALZET osmotic pump to simulate the tumor secretion of proinflammatory cytokines.

In conclusion, this study reported that IL-1α activates pericytes through the IL-1R1-related signaling pathway and then causes pituitary fibrosis, finally leading to decreased GH levels in aCP. Blocking this process can improve GH secretion. These findings reveal the pivotal role of IL-1α in regulating GH secretion. IL-1R1 in pericytes may be an important target for reversing or delaying the fibrosis of the pituitary gland in aCP.

Author contributions statement

Jian Mao, Binghui Qiu, Fen Mei performed primary data analysis and wrote the manuscript. Jian Mao, Fan Liu, Zhanpeng Feng performed experimental work related to animal preclinical studies. Jian Mao, Jun Fan, Jing Nie performed Immunofluorescence and ELISA. Jian Mao, Lijun Huang, Xixian Liao, Zhenhao Wang, Jiahui Zeng, Zelin Weng, Nailiang Zang performed H&E, Western blot and immunohistochemistry. Songtao Qi, Yun Bao designed and supervised the study. All authors edited and approved the final manuscript.

Funding

This study was supported by National Science and Technology Infrastructure Program (2014BAI04B01), Science and Technology Planning Project of Guangdong Province, China (2016A020213006), Chinese National Natural Science Foundation (81701197), Natural Science Foundation of Guangdong Province (2017A030310111), President Foundation of Nanfang Hospital, Southern Medical University (2017B009, 2018C017).

Declaration of competing interest

The authors declare no conflict of interest.

References

[1] Muller HL. Craniopharyngioma. Endocr Rev 2014;35:513–43.
[2] Hayashi M, Tomobe K, Hoshimoto K, Ohkura T. Successful pregnancy following gonadotropin therapy in a patient with hypogonadotropic hypogonadism resulting from craniopharyngioma. Int J Clin Pract 2002;56:149–51.
[3] Boekhoff S, Bogusz A, Sterkenburg AS, Eveslage M, Muller HL. Long-term effects of growth hormone replacement therapy in childhood-onset craniopharyngioma: results of the German Craniopharyngioma Registry (HIT-Endo). Eur J Endocrinol 2018;179:331–41.
[4] Tosta-Hernandez PDC, Siviero-Miachon AA, da Silva NS, Cappellano A, Pinheiro MM, Spinola-Castro AM. Childhood craniopharyngioma: a 22-year challenging follow-up in a single center. Horm Metab Res 2018;50:675–82.
[5] Tomlinson JW, Holden N, Hills RK, Wheatley K, Clayton RN, Bates AS, et al. Association between premature mortality and hypopituitarism. West midlands prospective Hypopituitary study group. Lancet 2001;357:425–31.
[6] Diez JJ, Gomez-Pan A, Iglesias P. Towards a concept of growth hormone deficiency syndrome in adults. Med Clin 1996;107:218–23.
[7] Diez JJ. The syndrome of growth hormone deficiency in adults: current criteria for the diagnosis and treatment. Med Clin 2000;114:468–77.
[8] Corpas E, Harman SM, Blackman MR. Human growth hormone and human aging. Endocr Rev 1993;14:20–39.
[9] Li K, Lu X, Yang N, Zheng J, Huang B, Li L. Association of pituitary stalk management with endocrine outcomes and recurrence in microsurgery of craniopharyngiomas: a meta-analysis. Clin Neurol Neurosurg 2015;136:20–4.
[10] Daubenbuchel AM, Muller HL. Neuroendocrine disorders in pediatric craniopharyngioma patients. J Clin Med 2015;4:389–413.
[11] Gan HW, Phipps K, Aquilina K, Gaze MN, Hayward R, Spoudeas HA. Neuroendocrine morbidity after pediatric optic gliomas: a longitudinal analysis of 166 children over 30 years. J Clin Endocrinol Metab 2015;100:3787–99.
[12] Arafah BM, Nasrallah MP. Pituitary tumors: pathophysiology, clinical manifestations and management. Endocr Relat Cancer 2001;8:287–305.
[13] Nie J, Huang GL, Deng SZ, Bao Y, Liu YW, Feng ZP, et al. The purine receptor P2X7R regulates the release of pro-inflammatory cytokines in human craniopharyngioma. Endocr Relat Cancer 2017;24:287–96.
[14] Zhou J, Zhang C, Pan J, Chen L, Qi ST. Interleukin6 induces an epithelialmesenchymal transition phenotype in human adamantinomatous craniopharyngioma cells and promotes tumor cell migration. Mol Med Rep 2017;15:4123–31.
[15] Gleason TH, Stebbins PL, Shanahan MF. Lymphoid hypophysitis in a patient with hypoglycemic episodes. Arch Pathol Lab Med 1978;102:46–8.
[16] Carpinteri R, Patelli I, Casanueva FF, Giustina A. Pituitary tumours: inflammatory and granulomatous expansive lesions of the pituitary. Best Pract Res Clin Endocrinol Metab 2009;23:639–50.
[17] Joshi MN, Whitelaw BC, Palomar MT, Wu Y, Carroll PV. Immune checkpoint inhibitor-related hypophysitis and endocrine dysfunction: clinical review. Clin Endocrinol (Oxf) 2016;85:331–9.
[18] Chang LS, Barroso-Sousa R, Tolaney SM, Hodi FS, Kaiser UB, Min L. Endocrine toxicity of cancer immunotherapy targeting immune checkpoints. Endocr Rev 2019;40:17–65.
[19] Van Linthout S, Miteva K, Tschope C. Crosstalk between fibroblasts and inflammatory cells. Cardiovasc Res 2014;102:258–69.
[20] Sano T, Kovacs KT, Scheithauer BW, Young Jr WF. Aging and the human pituitary gland. Mayo Clin Proc 1993;68:971–7.
[21] Dho YS, Kim YH, Se YB, Han DH, Kim JH, Park CK, et al. Endoscopic endonasal approach for craniopharyngioma: the importance of the relationship between pituitary stalk and tumor. J Neurosurg 2018;129:611–9.
[22] Bijkerk R, Au YW, Stam W, Duijs J, Koudijs A, Lievers E, et al. Long non-coding RNAs rian and miat mediate myofibroblast formation in kidney fibrosis. Front Pharmacol 2019;10:215.
[23] Ho KK, Participants GHDCW. Consensus guidelines for the diagnosis and treatment of adults with GH deficiency II: a statement of the GH Research Society in association with the European Society for Pediatric Endocrinology, Lawson Wilkins Society, European Society of Endocrinology, Japan Endocrine Society, and Endocrine Society of Australia. Eur J Endocrinol 2007;157:695–700.
[24] Frei K, Gramatzki D, Tritschler I, Schroeder JJ, Espinoza L, Rushing EJ, et al. Transforming growth factor-beta pathway activity in glioblastoma. Oncotarget 2015;6:5963–77.
[25] Fry C, Gunter DR, McMahon CD, Steele B, Sartin JL. Cytokine-mediated growth hormone release from cultured ovine pituitary cells. Neuroendocrinology 1998;68:192–200.
[26] Kondo M, Yamato M, Takagi R, Namiki H, Okano T. The regulation of epithelial cell proliferation and growth by IL-1 receptor antagonist. Biomaterials 2013;34:121–9.
[27] Rodriguez LG, Wu X, Guan JL. Wound-healing assay. Methods Mol Biol 2005;294:23–9.
[28] Mao J, Bao Y, Mei F, Liao X, Liu F, Zhou L, et al. An improved method of culturing somatotropic cells from rat adenohypophysis. Tissue Cell 2019;58:93–8.
[29] Kim B, Lee Y, Kim E, Kwak A, Ryoo S, Bae SH, et al. The interleukin-1alpha precursor is biologically active and is likely a key alarmin in the IL-1 family of cytokines. Front Immunol 2013;4:391.
[30] Kanehisa M, Sato Y, Furumichi M, Morishima K, Tanabe M. New approach for understanding genome variations in KEGG. Nucleic Acids Res 2019;47:D590–5.
[31] Sun YB, Qu X, Caruana G, Li J. The origin of renal fibroblasts/myofibroblasts and the signals that trigger fibrosis. Differentiation 2016;92:102–7.
[32] Fujiwara K, Jindatip D, Kikuchi M, Yashiro T. In situ hybridization reveals that type I and III collagens are produced by pericytes in the anterior pituitary gland of rats. Cell Tissue Res 2010;342:491–5.
[33] Tsukada T, Azuma M, Horiguchi K, Fujiwara K, Kouki T, Kikuchi M, et al. Folliculostellate cell interacts with pericyte via TGFbeta2 in rat anterior pituitary. J Endocrinol 2016;229:159–70.
[34] Ranke MB, Wit JM. Growth hormone - past, present and future. Nat Rev Endocrinol 2018;14:285–300.
[35] Roepke TK, King EC, Reyna-Neyra A, Paroder M, Purtell K, Koba W, et al. Kcne2 deletion uncovers its crucial role in thyroid hormone biosynthesis. Nat Med 2009;15:1186–94.
[36] Neuhaus JF, Baris OR, Kittelmann A, Becker K, Rothschild MA, Wiesner RJ. Catecholamine metabolism induces mitochondrial DNA deletions and leads to severe adrenal degeneration during aging. Neuroendocrinology 2017;104:72–84.

[37] Di Paolo NC, Shayakhmetov DM. Interleukin 1alpha and the inflammatory process. Nat Immunol 2016;17:906–13.
[38] Karanth S, McCann SM. Anterior pituitary hormone control by interleukin 2. Proc Natl Acad Sci U S A 1991;88:2961–5.
[39] Rivier C. Does IL-6 release ACTH by exerting a direct effect in the rat anterior pituitary. Stress 2001;4:39–55.
[40] Szalecki M, Malinowska A, Prokop-Piotrkowska M, Janas R. Interactions between the growth hormone and cytokines - a review. Adv Med Sci 2018;63:285–9.
[41] Renner U, Newton CJ, Pagotto U, Sauer J, Arzt E, Stalla GK. Involvement of interleukin-1 and interleukin-1 receptor antagonist in rat pituitary cell growth regulation. Endocrinology 1995;136:3186–93.